metals

MDPI

Article

The Defect Structure Evolution in MgH_2-EEWNi Composites in Hydrogen Sorption–Desorption Processes

Viktor N. Kudiiarov, Alan Kenzhiyev *, Roman R. Elman, Nikita Kurdyumov, Ivan A. Ushakov, Andrei V. Tereshchenko, Roman S. Laptev, Mark A. Kruglyakov and Parvizi I. Khomidzoda

Division for Experimental Physics, School of Nuclear Science & Engineering, National Research Tomsk Polytechnic University, 634050 Tomsk, Russia; kudiyarov@tpu.ru (V.N.K.); rre1@tpu.ru (R.R.E.); nek6@tpu.ru (N.K.); jiaozu@tpu.ru (I.A.U.); nwb@tpu.ru (A.V.T.); laptevrs@tpu.ru (R.S.L.); kruglyakov97@tpu.ru (M.A.K.); pih1@tpu.ru (P.I.K.)

* Correspondence: kenzhiyev@tpu.ru; Tel.: +7-999-178-2720

Abstract: This paper presents the results of the study of the composite based on magnesium hydride with the addition of nanosized nickel powder, obtained by the method of an electric explosion of wires. The obtained MgH_2-EEWNi (20 wt.%) composite with the core-shell configuration demonstrated the development of a defect structure, which makes it possible to significantly reduce the hydrogen desorption temperature from 418 °C for pure magnesium hydride to 229 °C for hydride with the addition of nickel powder. In situ studies of the evolution of the defect structure using positron annihilation methods and diffraction methods made it possible to draw conclusions about the influence of the $Mg_2NiH_{0.3}$ and Mg_2NiH_4 phases on the sorption and desorption properties of the composite. The results obtained in this work can be used in the field of hydrogen energy in mobile or stationary hydrogen storage systems.

Keywords: hydrogen storage material; magnesium hydride; nickel; nanoscale powders; hydrogen; desorption

Academic Editor: Qing Shu

Received: 24 December 2024
Revised: 12 January 2025
Accepted: 13 January 2025
Published: 16 January 2025

Citation: Kudiiarov, V.N.; Kenzhiyev, A.; Elman, R.R.; Kurdyumov, N.; Ushakov, I.A.; Tereshchenko, A.V.; Laptev, R.S.; Kruglyakov, M.A.; Khomidzoda, P.I. The Defect Structure Evolution in MgH_2-EEWNi Composites in Hydrogen Sorption–Desorption Processes. *Metals* **2025**, *15*, 72. https://doi.org/10.3390/met15010072

1. Introduction

Metal-hydrogen systems have their own specific features, which are associated mainly with the high diffusion mobility of hydrogen in the crystal lattice of metals and their alloys, as well as high reactivity. This is due to the fact that hydrogen tends to interact with various types of defects, such as impurity atoms, dislocations, grain boundaries, vacancy-type defects, and its own embedding atoms [1–7]. Hydrogen can induce the formation of many other defects and actively interact with defects in the structure of the material as well. Many studies have been aimed at studying the effect of hydrogen on defects, their structure and mechanical properties, but the mechanisms of such influence have not been fully established and explained. Thus, it is important to develop and improve known methods for defect control in functionally graded materials. This is directly related to the unresolved problems of the hydrogen embrittlement of metals, which is why many scientific works are devoted to the creation of completely new materials for operation in a hydrogen environment [8–16]. In this context, the most effective method for evaluating hydrogen interaction with the structure of defects is the positron spectroscopy method. Due to its high sensitivity, it allows the most accurate determination of the type of defects and their concentration, as well as the chemical environment. The effectiveness of this method has been demonstrated in many studies [17–20].

Another area of application for positron spectroscopy may be hydrogen storage materials. Since hydrogen stored in hydride-forming materials is currently considered as a promising energy carrier, it is important to study the properties of the interaction of such materials with hydrogen. Of particular interest in this case is the study of metal hydrides with different properties [21–27]. One of the most common hydride-forming materials is $LaNi_5$. This compound is characterized by high cyclic stability and is capable of absorbing and releasing about (1.2–1.4) wt.% hydrogen at room or higher temperatures. This makes it suitable for use in laboratory storage devices. However, this compound has disadvantages, such as high cost and mass, as well as limited production sites. Due to the small capacity for storing hydrogen, the possibilities of using this hydrogen storage material are limited. Another promising hydrogen storage material is magnesium. Magnesium hydride has several advantages: it is light, cheap, and has a high hydrogen capacity (7.6% by weight). However, it has a few drawbacks as well. It has a high bond stability with hydrogen and begins to dissociate only at relatively high temperatures of about 400 °C. Despite the slow kinetics and high activation energy of desorption, this material is of great interest to researchers as a potential mobile source of hydrogen storage. To improve the properties of magnesium hydride, the authors of various studies suggest using different methods and approaches [28–36]. One of the most well-known methods for improving sorption characteristics is milling in a planetary ball mill. This method allows the magnesium powder to be activated by mechanical friction [37–42]. Activation in this case means the mechanical milling of the powder in order to destroy the oxide layer and increase the surface area to create additional hydrogen diffusion paths into the bulk of the material. Moreover, the interaction of magnesium and hydrogen is strongly influenced by the presence of various catalysts that can be added during the ball milling process. However, the grinding process in a ball mill is inextricably linked with the occurrence of a defective structure. In addition, catalytic additives affect both the formation of defects during the ball milling process and the evolution of the defect structure during the hydrogen sorption/desorption processes.

When considering magnesium hydride, catalytic additives are one of the most common methods for improving hydrogen storage properties. In recent years, many research papers have been published on the effects of catalytic additives on magnesium hydride by various research groups. Metal oxides are most often used as additives [43–45], as well as transition metals: nickel [46,47], cobalt [48], iron [49], titanium [50], vanadium [51], palladium [52], rare earth metals [53,54], etc. However, the problem of reducing operating temperatures is still relevant. Many authors [54–62] note an acceptable level of reduction in operating temperature and maximum hydrogen performance by using Ni as additive material to MgH_2. Doppiu S., Schultz L., and Gutfleisch O. [60], in their work, obtained a composite based on magnesium hydride with the addition of nickel obtained by the decomposition of metal carbonyl. All catalysts were divided into micro-, submicro-, and nano-nickel. According to the data obtained, the most effective added material turned out to be a powder with a nano-nickel configuration. This effect was explained by the size of the added powder materials; in this case, the dependence on the size factor was demonstrated. Liang G. et al. [61], in a similar work, investigated the effect of adding another metal group, such as Ti, V, Mn, Fe, or Ni. The result of the work was that the addition of only 1 at.% nickel reduces the temperature of hydrogen desorption from 450 °C to 350–370 °C. Shang et al. [62] conducted their own research, and according to the results, they were able to establish that the addition of 8 mol.% nickel allows the magnesium hydride to dissociate at temperatures of about 300 °C. They associate this phenomenon with the formation of the intermetallic hydride phase Mg_2NiH_4. In their work, desorption kinetics were rapidly achieved, in ~700–800 s. Thus, great progress has been made in the study of magnesium hydride with the addition of nickel, but no attention has been paid to the study of the defect

structure of the resulting compositions. Moreover, nano-nickel produced by the electrical explosion method has also not been sufficiently studied as a catalytic additive to MgH_2.

It is important to note that complex defect structure is formed in the composite when magnesium hydride and EEWNi are milled together in a planetary ball mill. This defective structure can have a significant impact on the interaction of the composite with hydrogen. The presence of a catalytic additive can also already affect the defective structure in the processes of hydrogen sorption and desorption. At the same time, the method of positron annihilation spectroscopy is the only method that allows the direct study of the influence of defects on the processes of hydrogen sorption/desorption for hydrogen storage materials. Thus, in this work, for the first time, a comprehensive analysis was carried out on a specially designed spectrometric complex that combines an automated system for studying the interaction of hydrogen with materials (Sievert's type) and positron spectroscopy to determine the effect of the defect structure of the composite based on MgH_2 and EEWNi on its interaction with hydrogen. Thus, the novelty of this study is the comprehensive approach to the study of the Mg–EEWNi–H hydrogen storage system, including in situ methods of positron annihilation.

2. Materials and Methods

2.1. Materials Preparation

Nanoscale nickel powder obtained by the electric explosion of wires (EEWNi) [63–66] and magnesium of MPF-4 grade (NMK Ural, Yekaterinburg, Russia) of a high purity of 99.2% with a particle size of 50–300 μm were used to obtain the composite. Magnesium powder was preliminarily subjected to mechanical activation in a planetary ball mill and then to hydrogenation using the Gas Reaction Automated Machine (GRAM) complex (Tomsk Polytechnic University, Tomsk, Russia). A detailed description of the mechanical activation and hydrogenation process are presented in [67]. They are acceptable and optimal for the synthesis of this type of powder materials. The mechanical synthesis of composites was carried out in planetary ball mill AGO-2 (NPO NOVIC LLC, Novosibirsk, Russia) at the following parameters: jar rotation speed was 900 rpm, milling time was 120 min, the mass ratio of balls to powder was 20:1, and the amount of EEWNi powder was 20 wt.%. To eliminate the possibility of contamination and appearance of oxides on the surface of the materials used, the processes of unpacking the packages and loading into the drums of the planetary ball mill and chambers of the automated complex were carried out in a sealed glove box, SPEX GB 02M (Spectroscopic Systems, Lomonosov Moscow State University, Moscow, Russia), with an argon supply line to the working chamber and airlock. The contents of purified argon 99.999%, water vapor, and oxygen were less than 1 ppm.

2.2. Analysis and Characterization

The morphology of the obtained composites was studied using a TESCAN VEGA 3 SBU scanning electron microscope (Tescan Orsay Holding s.r.o., Brno, Czech Republic). The elemental composition of the composite was analyzed by the energy-dispersive X-ray spectroscopy on an XMax 50 X-ray spectrometer (Oxford Instruments plc, Abingdon, UK). Transmission electron microscopy (TEM) was performed on a Philips CM12 microscope (Philips/FEI Company, Amsterdam, The Netherlands/Hillsboro, OR, USA). Differential scanning calorimetry was carried out on a STA 449 F3 Jupiter unit (Netzsch, Selb, Germany). Hydrogen concentration curves and hydrogen sorption–desorption cycles were obtained using a Gas Reaction Automated Machine (GRAM) complex specially developed at the Department of Experimental Physics of Tomsk Polytechnic University. Hydrogen concentration was measured after hydrogen sorption–desorption experiments by melting the sample in an inert gas (Ar) atmosphere using an RHEN602 hydrogen analyzer (LECO

Corporation, St. Joseph, MI, USA). The crystalline structure of the samples was analyzed by X-ray diffraction (XRD) in the scanning range of (5–80)° using an XRD-7000S (Shimadzu, Kyoto, Japan). The diffractometer was operated in a Bragg-Brentano configuration with a Cu Kα tube (λ = 0.154 nm, 40 kV, 30 mA) with a divergence slit of 1 mm. The study of phase transitions in magnesium hydride and the composite during dehydrogenation was carried out in situ at the Precision Diffractometry II station of the Institute of Nuclear Physics, Siberian Branch of the Russian Academy of Sciences, on channel 6 of the synchrotron radiation of the VEPP-3 electron storage ring. Single-coordinate detectors simultaneously record the scattered radiation in a specified angular range (~30°) over 3328 channels at a rate of up to 10 MHz. The sample was placed in a chamber pumped with argon to remove air, and the sample was heated linearly to a temperature of 723 K at a rate of 6 K/min. The analysis of the gas release during temperature-programmed desorption was performed using a UGA100 mass spectrometer (Stanford Research Systems, Sunnyvale, CA, USA). The measured diffraction patterns were processed and reflections were identified using the PDF-2 (2004) database, FullProf Suite (Version 5.20), and Crystallographica (Version 2.1.1.1 Copyright © 1996–2004 Oxford Cryosystems) search-match software. The in situ analysis of experimental samples of magnesium powders and composites based on these was carried out using the Doppler broadening spectroscopy method on a specialized facility [68]. A positron source based on the ^{64}Cu isotope was used in this work. This source can be produced by the reaction ^{63}Cu (n, γ) $\rightarrow$ ^{64}Cu by irradiating copper foil with a thermal neutron flux. Pure copper, which has a high melting point, interacts very weakly with hydrogen compared to other materials, allowing it to be used in a heated hydrogen environment at high pressure [34]. DBS were acquired and recorded every five minutes. The minimum number of spectra in each sample was 150,000. The ratio of the number of positron events at the center of the annihilation peak to the total number of events below the peak is known as the S parameter and characterizes the probability of positron annihilation with free electrons. The parameter W is defined as the ratio of the number of events in the wings of the annihilation peak to the total area of the peak and characterizes the probability of positron annihilation with electrons. The S parameter is therefore more sensitive to changes in the free volume, while the W parameter is more sensitive to the chemical environment. The values used to determine S and W are as follows: channel width for S is 6; channel width for W is 8; parameter A is 40; and background level is 500 [34].

3. Results and Discussion

3.1. Composite Characterization

Figure 1 shows microphotographs of magnesium hydride and the MgH_2–20 wt.% EEWNi composite obtained using a scanning electron microscope (SEM), as well as particle size distribution histograms and element distribution maps.

Magnesium hydride particles represent large agglomerates up to 180 μm in size and consist of smaller particles of (3–15) μm in size as can be seen in the Figure 1e. The average particle size is about 12 μm (Figure 1e). At the same time, no contaminants are observed on the surface of the particles, and the elemental distribution map for this sample shows only the presence of the Mg (Figure 1b). SEM micrographs of the composite show that the particles of the synthesized MgH_2-EEWNi composite reach sizes of (0.08–0.18) μm (Figure 1c,f). The average particle size is much smaller than that of magnesium hydride and is about 0.14 μm (Figure 1f). The elemental distribution maps showed that during the mechanical synthesis process, nickel powder particles were uniformly distributed over the volume of the composite and deposited on magnesium particles (Figure 1d).

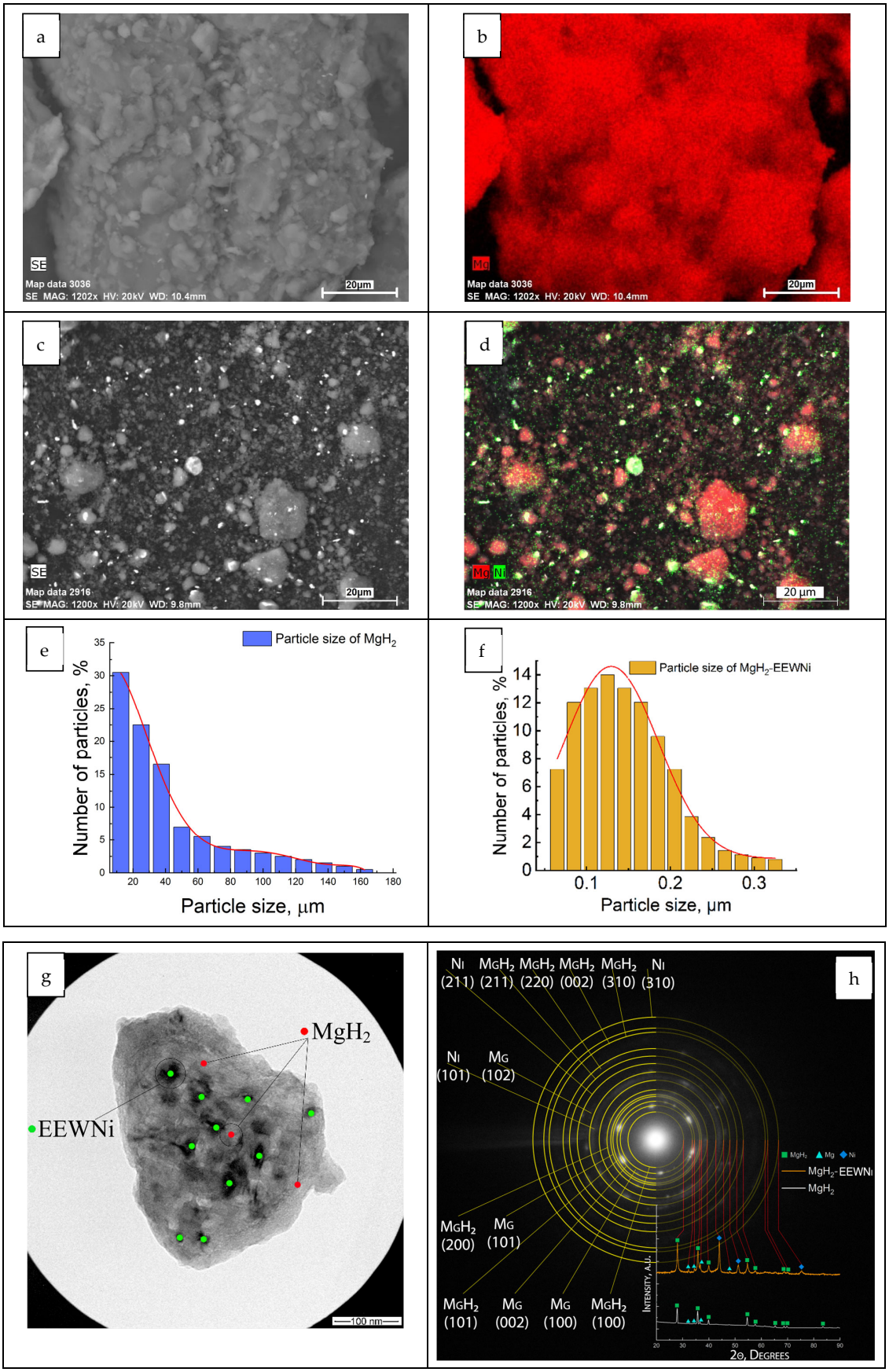

Figure 1. SEM micrographs of MgH_2 (**a**,**b**) and the MgH_2-EEWNi composite (**c**,**d**) with the corresponding elemental mapping analysis (**b**,**d**) and particle size distribution for MgH_2 (**e**) and composite (**f**), TEM image of the MgH_2-EEWNi composite particle (**g**), and the corresponding SAED pattern (**h**).

Figure 1g–h demonstrates the results obtained by transmission electron microscopy. From the images presented, the nanoscale nickel particles lying on the surface of the magnesium hydride particle can be clearly identified (Figure 1g). Thus, the composite particles represent a core-shell structure, where Ni nanoparticles acts as the shell and MgH_2 particles act as the core. The selected area electron diffraction (SAED) pattern demonstrated in Figure 1h makes it possible to conclude that there is no interaction between Mg and Ni with the formation of new phases. The diffraction rings and spots can be assigned to the Mg, MgH_2, and Ni phases. A small halo is observed at angles characteristic of magnesium hydride as well, which may indicate the formation of a small amount of amorphous phase during the milling process. The results of calculations of the sizes of coherent scattering regions and micro-stresses in MgH_2 and the MgH_2-EEWNi composite are presented in Table 1.

Table 1. Results of determining the sizes of coherent scattering regions and micro strains in magnesium hydride and MgH_2-EEWNi.

Sample	Phase	Phase Content, vol.%	Crystallite Size, nm	Strains, $\times 10^{-3}$
MgH_2	Mg	24	90	0.31
	MgH_2	76	70	2.32
MgH_2-EEWNi	Mg	18	31	1.76
	MgH_2	61	24	3.53
	Ni	21	31	3.84

The combined mechanical milling of magnesium hydride and EEWNi powder leads to a decrease in the size of crystallites and an increase in micro strains in all detected phases, since EEWNi particles are not only deposited on the surface of MgH_2 particles, but also embedded in the surface, inducing intense defect formation (this can be seen in the TEM image in Figure 1g), which also increases the milling efficiency. Higher stress values in the composite compared to magnesium hydride indicate the formation of a developed defect structure in the composite. In this regard, the use of positron spectroscopy to identify the features of defect formation in the composite and its interaction with hydrogen is relevant.

3.2. Hydrogen Storage Properties of the Composite

Figure 2 shows the differential scanning calorimetry (DSC) analysis of MgH_2 and the MgH_2-EEWNi composite when heated to 600 °C at a heating rate of 6 K/min in an inert gas (argon) stream. Differential scanning calorimetry (DSC) is a well-established technique in which the difference in the amount of heat needed to raise the temperature of a sample and a reference is measured as a function of temperature. Both the sample and the reference are maintained at almost the same temperature throughout the experiment. As a rule, the temperature program for DSC analysis is designed in such a way that the temperature of the sample holder increases linearly as a function of time. The control sample must have a well-defined heat capacity in the temperature range to be scanned.

The hydrogen yielding process from the composite was characterized by the presence of a peak at 229 °C, and compared to magnesium hydride the difference was 189 °C. The process of hydrogenation and dehydrogenation is accompanied by the process of the dissociation of hydrogen molecules at the surface of the material due to nickel powder particles covering magnesium hydride and acting as a "hydrogen pump", which make it easy to diffuse into the volume of the material. Figure 3a shows the X-ray diffraction (XRD) pattern of the corresponding composite after the dehydrogenation process.

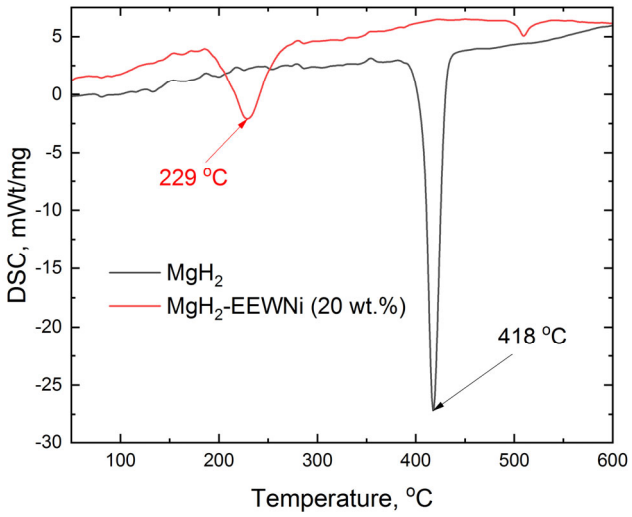

Figure 2. Differential scanning calorimetry (DSC) analysis of MgH_2 and the MgH_2-EEWNi composite.

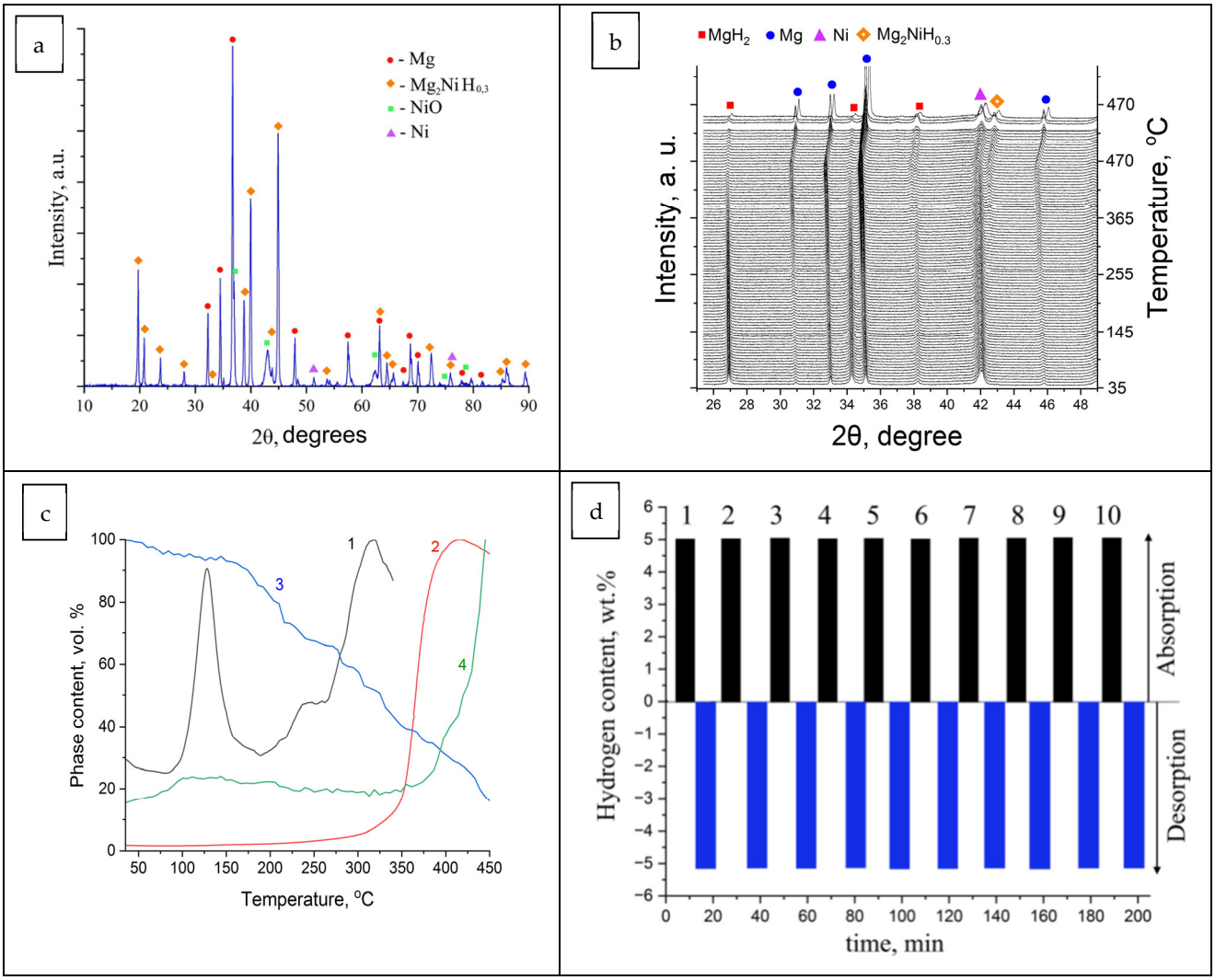

Figure 3. XRD pattern of the MgH_2-EEWNi sample after dehydrogenation (**a**), XRD pattern, obtained in situ during heating (**b**), graph of phase transformations during heating: 1—thermal-stimulated desorption for the composite MgH_2-EEWNi, 2—thermal-stimulated desorption for MgH_2, 3—decrease in the MgH_2 phase, and 4—increase in the Mg phase (**c**), and hydrogen sorption–desorption cycle test for the composite MgH_2-EEWNi (**d**).

From Figure 3b, it is clearly seen that an increase in the $Mg_2NiH_{0.3}$ phase can be observed, indicating the dissociation of magnesium hydride due to the introduction of nickel powder. Peaks of nickel and its oxide are observed as well, which is in agreement with the above presented data. Upon hydrogenation, the phase changes to Mg_2NiH_4 and acts as a "hydrogen pump". Nanoscale particles of nickel and its oxide act as additional hydrogen diffusion pathways. In situ studies using synchrotron radiation techniques can demonstrate the hydride phase change during desorption. Figure 3c clearly shows the dissociation of hydride during its heating, with a decrease in the hydride phase and an increase in the metal phase, in this case magnesium, with increasing temperature. Before the first temperature maximum, the dissociation of the material begins to occur, which allows us to complete the assumption about the mechanism of the "hydrogen pump" and the catalytic effect from the addition of nickel powder produced by the electrical explosion of the conductor. Experiments were also carried out to determine the cyclic stability of the composite, which is shown in Figure 3d. As a result of this experiment, it was found that during 10 sorption/desorption cycles, the composite demonstrates good cyclic stability and practically does not lose its hydrogen capacity. In the process of hydrogen sorption by magnesium without the addition of a catalyst, hydrogen molecules dissociate into individual atoms on the surface of the magnesium particle when overcoming a potential barrier under the influence of temperature and pressure, binding to atoms of the storage material, forming hydrides. In this case, a hydride layer is formed on the surface of the magnesium particle, which prevents the diffusion of hydrogen into the volume of the metal matrix. The hydrogen desorption process for magnesium hydride consists in the recombination of hydrogen atoms into a molecule on the surface of the particle, followed by the desorption of hydrogen from the volume. In the MgH_2-EEWNi composite, nickel and nickel oxide particles lying on the surface of magnesium particles have a significant catalytic effect, as a result, hydrogen molecules dissociate at temperatures below 473 K. It is known that Ni forms a Mg_2Ni intermetallic compound during hydrogenation, which then passes into Mg_2NiH_4 during hydrogen sorption, accelerating the diffusion of hydrogen into the volume of the material. At the same time, during desorption, individual hydrogen atoms recombine into molecular hydrogen, passing through nickel particles, and are desorbed from the surface of MgH_2 particles. It is shown that the hydrogen content in the initial composite MgH_2-EEWNi has an average value of ~4.64 wt.%. In the powder MgH_2-EEWNi after vacuum degassing, the hydrogen content is slightly lower (~4.46 wt.%), probably due to the removal of residual gases and water vapor. In the MgH_2-EEWNi composite, after thermal desorption, the residual hydrogen content is ~ 4% of the initial concentration. For further in situ analysis of the MgH_2-EEWNi composite, the absorption and backscattering coefficients of positrons and the path of positrons in this material were calculated (Table 2).

Table 2. Calculation of the absorption and backscattering coefficients of positrons and the path of positrons in a MgH_2-EEWNi composite.

Sample	Thickness, μm	The Backscattering Coefficient of Positrons	The Absorption Coefficient of Positrons, cm^{-1}	Intensity Without Taking into Account the Contribution of the Source
MgH_2–20 wt.%-EEWNi	5000	0.25	73	50
Copper source (^{64}Cu)	10	0.35	345	-
MgH_2–20 wt.%-EEWNi	5000	0.25	73	50

According to the calculations, filling a powder layer of more than 5 mm ensures the complete absorption of positrons from a source based on the isotope ^{64}Cu by the material

under study. In addition, as shown in Section 1, the distance from the edge of the source to the inner wall of the crucible of the experimental chamber should also exceed 5 mm. Thus, for in situ analysis of MgH_2-EEWNi composite powders, a round-shaped positron source of ∅4 mm is required. In this case, its mass will be ~ 1.5 g, which increases the irradiation time to achieve nominal activity to 120 ± 15 min. The in situ Doppler Broadening Spectroscopy (DBS) spectra are analyzed by estimating the S and W parameters for each spectrum as pressure and temperature change over time. Such a graphical representation is optimal because it provides information about the pulse distribution of positron annihilation in the material under study at each moment of time at a known pressure and temperature, which allows us to characterize the kinetics of processes and structural features quite fully. In situ studies by using positron annihilation methods for Mg/MgH_2 were performed in our previous articles [69,70]. The time dependences of pressure, temperature and DBS parameters for the composite MgH_2-EEWNi when held in vacuum at room temperature are shown in Figure 4.

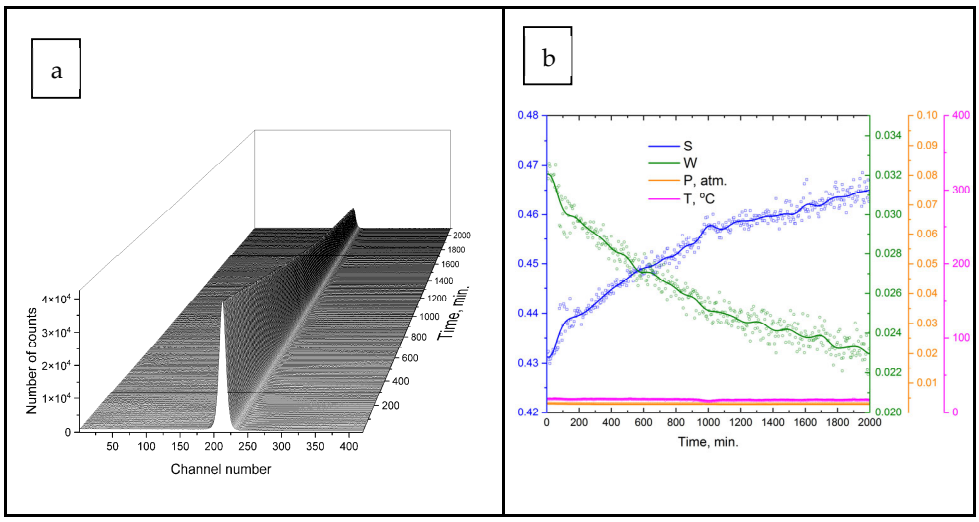

Figure 4. DBS in situ spectra (**a**) and dependencies S(t), W(t), P(t), and T(t) (**b**) for the MgH_2-EEWNi composite after exposure to a vacuum at room temperature.

According to the data presented in Figure 4a, in situ DBS spectra, there is a decrease in the number of samples over time associated with a change in the activity of the positron source. The activity of the ^{64}Cu isotope decreases markedly throughout the experiment due to its short half-life of ~12.5 h. The annihilation line narrows over time due to a decrease in half-width at half-height and a decrease in background with a significant decrease in overall statistics. The exposure of the MgH_2-EEWNi composite to a vacuum at room temperature is accompanied by an increase in the S parameter and a corresponding decrease in the W parameter due to the stabilization of the detector load and a change in the recording efficiency. The W parameter reflects the fraction of positron annihilations with high-momentum electrons. For example, in the vicinity of a vacancy-type defect, the main contribution to the electron density comes from valence electrons around atoms, as a result of which the W parameter decreases and, accordingly, the S parameter becomes larger. The change in the S parameter reflects information about the annihilation of positrons on electrons with low momenta, i.e., on valence electrons (in metal conduction electrons serve as electrons with low momenta), which carry information about the structure of the energy band of the material and the Fermi surface located in the band. The dependence of the annihilation parameters for the MgH_2 sample showed similar changes over time [69]. Figure 5 shows the in situ DBS spectra and the corresponding dependences of pressure, temperature, and

S and W parameters for the composite MgH_2-EEWNi obtained by stepwise heating in a vacuum and in a hydrogen medium at pressures of 2 and 30 bar.

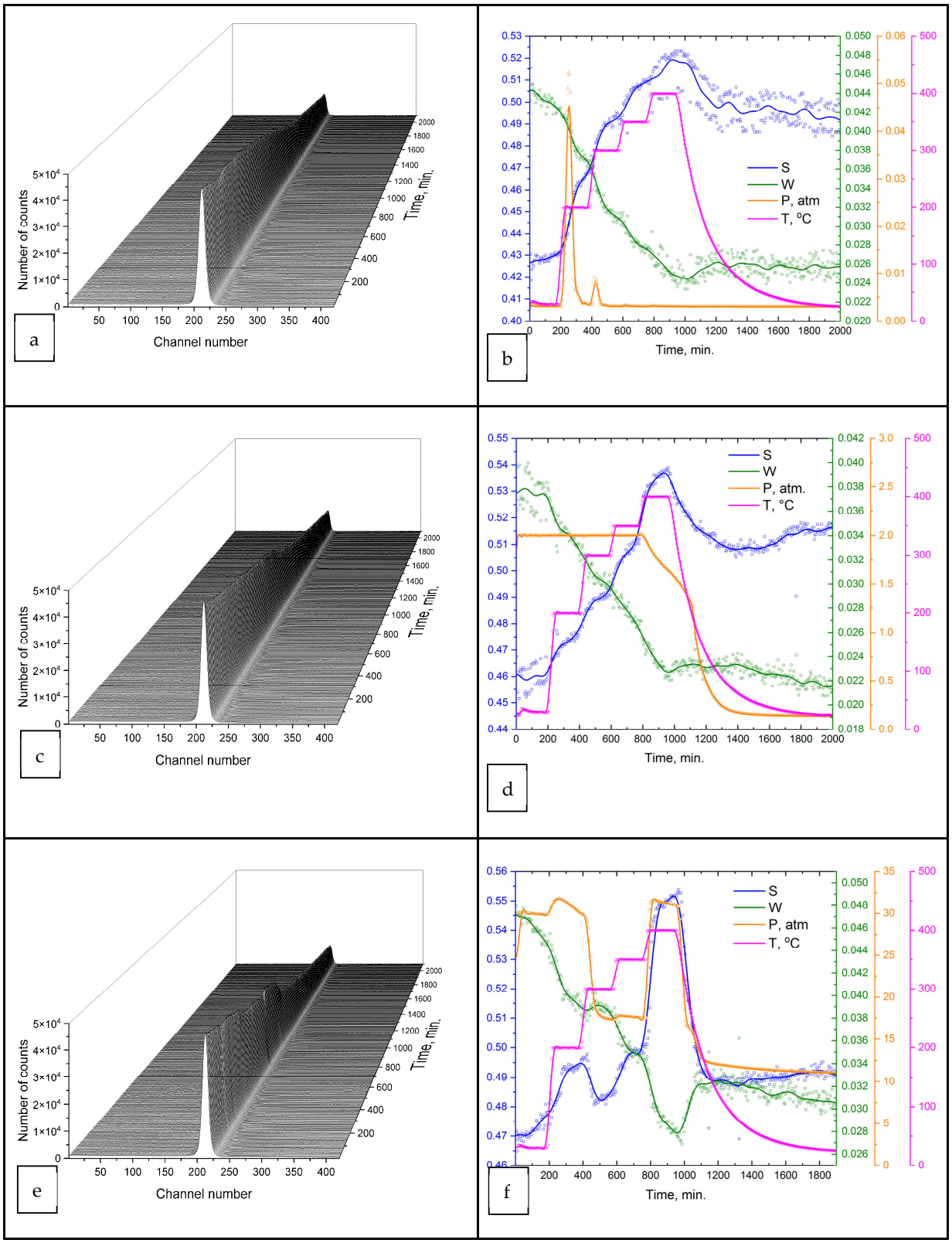

Figure 5. DBS in situ spectra and dependencies S(t), W(t), P(t), and T(t) for the MgH_2-EEWNi composite during vacuum heating (**a**,**b**), heating at 2 bar of hydrogen (**c**,**d**), and heating at 30 bar of hydrogen (**e**,**f**).

Significant changes in the shape of the annihilation lines are observed over a period of 200 to 1200 min during the thermally stimulated hydrogen desorption from the MgH_2-EEWNi composite. In situ DBS spectra during the thermally stimulated desorption of the composite (Figure 5a) reveal a sharp increase in the parameter S in the range from 200 to 500 min, which is associated with the intensive decomposition of hydrides and the release of hydrogen atoms from the material. Comparing these data with changes in pressure P and temperature T during this period (Figure 5b), the release of hydrogen from the composite in the time range of (190–300) min is accompanied by a sharp increase in the S parameter and a decrease in the W parameter, as well as a noticeable increase in pressure P. In the range corresponding to an increase in temperature from 50 to 200 °C, the changes are due to both the release of adsorbed gases from the surface of the MgH_2-EEWNi composite particles and the release of hydrogen as a result of the rapid decomposition of MgH_2. In the second range, corresponding to the time interval of (400–560) min, there is also an intense hydrogen yield, while for magnesium hydride only one broad and intense peak of hydrogen release was observed at (555–750) min upon reaching a temperature of (342–400) °C [69]. This second peak for the composite is associated with the decomposition of residual hydrides in the composite. The relative change in the parameter S in these two ranges is significantly higher, which confirms the intensive process of hydrogen desorption and the decomposition of hydrides in the specified time intervals. Such an intense change in the S parameter may indicate both an increase in the excess free volume in the material due to the dissociation of hydrogen-associated defects and an increase in the concentration of vacancy-type defects, and a change in the electronic structure. In particular, the transition from an "insulator" to a "metal" as a result of the decomposition of magnesium hydrides affects the concentration of charge carriers and the electronic structure of the material. A similar correlation was observed previously for MgH_2 and MgH_2-based composites [69,70]. The observed changes in the S and W parameters indicate the complex dynamics of physico-chemical processes during the heating of MgH_2-EEWNi in a vacuum, including hydrogen desorption and the evolution of the composite structure. The changes in the DBS parameters occur in stages and correspond to the heating profile with further heating. This profile is due to a combination of changes in the activity of the positron source and the formation of thermal vacancies in Mg. It is noted that the release of hydrogen at the high temperatures observed in the intervals of (600–630) and (780–810) min is associated with residual hydrogen, which is strongly associated with defects, as well as with a small amount of hydrides in the material that were not doped with the catalytic additive EEWNi. In the range of (950–2000) min, the composite sample is cooled to room temperature in a vacuum. Thus, the behavior of DBS parameters in the process of thermally stimulated desorption can be characterized in several stages. At the first stage, in the range of (0–190) min, a slight increase in the S parameter and a decrease in the W parameter are observed due to a decrease in the activity of the positron source. The second stage includes both ranges associated with the release of adsorbed gases and the decomposition of hydrides (stages with more abrupt changes in S and W parameters, ranges (190–300) and (400–560) min), as well as the contribution from changes in the activity of the source and the formation of thermal vacancies in the sample (contribution to the intervals at which the output is observed hydrogen, and the stages of a smoother change in the S and W parameters in the interval of 400–920 min). The third stage, (950–2000) min, is characterized by minor changes in the S and W parameters, while the contribution is mainly made by the relaxation of thermally induced defects (decrease in S parameter) and a change in the activity of the positron source (increase in S parameter). As a result of the exposure of the MgH_2-EEWNi composite to a hydrogen atmosphere at a pressure of 2 bar (Figure 5c,d), special changes in the shape of the annihilation line are observed, other than thermally stimulated desorption.

In this case, changes in the shape of the annihilation line are limited to a small number of counts during the first 1000 min. This is due to an increase in the free volume in the material during heating and holding at a constant temperature and pressure of hydrogen, as well as a change in the activity of the source. The graph of the dependencies of the DBS, temperature, and pressure parameters also confirms that these changes follow a complex stepwise heating profile. The exposure of the composite to a hydrogen atmosphere at a pressure of 2 bar in the first 500 min does not lead to hydrogen absorption or desorption by the material. There are no areas of sharp decrease in S and increase in W parameters during thermally stimulated desorption, which indicates the absence of phase transformations $Mg \rightarrow MgH_2$ and other induced physico-chemical processes in this time interval. Thus, at this stage of the process, there is mainly an accumulation of thermally induced defects, without observed phase changes in the material. However, it is worth noting that in the range of (300–920) min, there is a more significant increase in the S parameter and a decrease in the W. These changes become most significant in the range from 800 to 920 min, which indicates the accumulation of thermal and hydrogen-induced defects under the influence of elevated temperature and a hydrogen atmosphere. At the stage of subsequent cooling, (920–1400) min, there is a decrease in S and an increase in W parameters, which are due not only to the relaxation of defects at the initial stage of the cooling process with a decrease in the activity of the source, but also to the absorption of hydrogen and the phase transformation of $Mg \rightarrow MgH_2$. A further gradual increase in S parameter and a decrease in parameter W at (1400–2000) min is associated with a decrease in the contribution of defect relaxation and the presence of a larger contribution from changes in the activity of the ^{64}Cu isotope. The DBS in situ spectra for the MgH_2-EEWNi composite under exposure conditions at 30 bar of hydrogen (Figure 5e) exhibits a more complex shape compared to other patterns and includes several additional stages. Analyzing them in combination with pressure graphs for the corresponding measurements (Figure 5f), it can be noted that the number of counts increases during hydrogen desorption and decreases during sorption. This indicates that the shape of the annihilation line is closely related to the phase transformations in the magnesium–hydrogen system and the physico-chemical processes occurring during hydrogen sorption and desorption. The injection of 25 bar of hydrogen into the chamber at room temperature has a negligible effect on the DBS parameters, the nature of the dependencies of which is mainly due to a decrease in the activity of the positron source. The same effect was observed when magnesium was heated in hydrogen medium [70]. Heating to a temperature of 200 °C leads to an increase in pressure in the chamber to 32 bar; however, the intensive absorption of hydrogen by magnesium powder does not occur. However, a gradual, slow uptake of hydrogen was observed, in contrast to magnesium [70]. At the same time, there is an increase in the S parameter and a decrease in the W parameter. Heating to 300 °C in a time interval of (400–450) min leads to the beginning of an active hydrogen sorption process, accompanied by an increase in the parameter W and a decrease in the parameter S, and a phase transformation occurs with the formation of hydrides. Thus, active hydrogen absorption up to equilibrium was completed in two times less time than for Mg/MgH_2, which indicates a faster sorption rate [70]. Further exposure and an increase in temperature to 350 °C in the interval of (480–780) min leads to pressure equalization, but further hydrogen sorption does not occur. There is only a slight increase in pressure due to an increase in temperature from 300 °C to 350 °C. In this case, the parameter S increases and the parameter W decreases, which, apparently, is due to rapid diffusion in the volume of the material and the accumulation of hydrogen-induced defects. Heating to 400 °C is accompanied by a significant increase in pressure in the chamber due to hydrogen desorption and a sharp increase in the S parameter. In this range, not only the active accumulation of thermal and hydrogen-induced defects occurs, but also

the decomposition of hydrides, accompanied by an intensive release of hydrogen. There is also a transition of the electronic structure from an insulator (MgH_2) to a metal (Mg). Exposure at this temperature has practically no effect on the S and W parameters, or on the MgH_2 sample [70]. However, after that, the absorption of hydrogen is accompanied by the same sharp change in the parameter S in the opposite direction. Apparently, the Mg_2NiH_4–Mg_2Ni phase, which occurs during the processes of hydrogen sorption/desorption at a given hydrogenation pressure, as well as other structural-phase transformations, plays an important role here. The pressure of hydrogen in the chamber drops to 11 bar upon cooling, and the main stage of the phase transformation from magnesium to hydride occurs. In our earlier study, a composite based on magnesium hydride with the addition of aluminum powder obtained by electric wire explosion was prepared. The lowest desorption temperature from the MgH_2-EEWAl composite (10 wt.%) was 300 °C, compared to pure magnesium hydride—393 °C at a heating rate of 2 K/min. The mass content of hydrogen in the composite was 5.5 wt.%. The positive effect of the aluminum powder produced by the electric explosion of wires method on reducing the activation energy of desorption was demonstrated. The composite's desorption activation energy was found to be 109 ± 1 kJ/mol, while pure magnesium hydride had an activation energy of 161 ± 2 kJ/mol [71].

Figure 6 shows the scheme of the formation of the Mg_2NiH_4 and Mg_2Ni phases. A scheme for reducing the activation energy of desorption for the MgH_2-EEWNi composite is also presented here. This behavior in the interaction of hydrogen with the material is caused by the effect of adding nanoscale nickel powder and the co-milling of materials in a planetary ball mill.

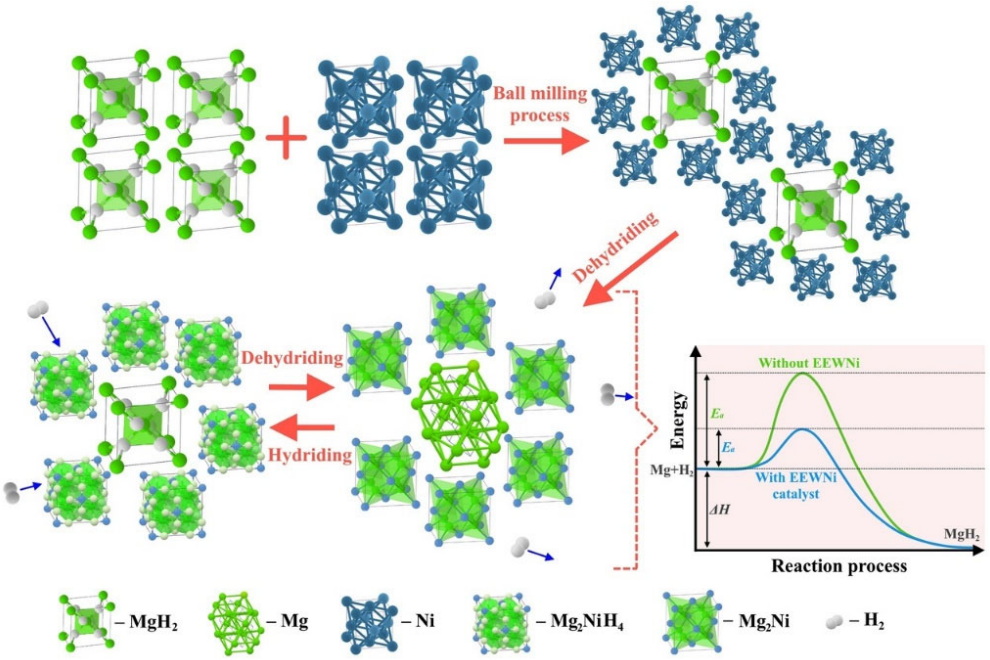

Figure 6. Schematic representation of the mechanism of reducing the activation energy of hydrogen desorption from the MgH_2-EEWNi composite.

The mechanism is as follows. The co-milling of magnesium hydride with nano-nickel leads to the formation of a core-shell structure, where Ni nanoparticles act as the shell and MgH_2 particles act as the core. Further, in the obtained composite in the processes of hydrogen sorption and desorption, additional phases are formed, which contribute to faster absorption and the release of hydrogen. During hydrogen sorption, the Mg_2Ni phase appears, which then, during the hydrogenation process, passes into the ternary hydride phase Mg_2NiH_x, which acts as a "hydrogen pump". The obtained results of in

situ positron spectrometry make it possible to identify mechanisms for improving the basic characteristics of hydrogen storage materials and to develop technological approaches to the formation and management of their structure.

4. Conclusions

In this work it was experimentally shown that the addition of nickel nanoparticles obtained by the electric explosion of wires significantly improves the hydrogen sorption and desorption properties of Mg/MgH_2. Using scanning electron microscopy, it was shown that the composite consists of MgH_2 particles and 20 wt.% of EEWNi nanoparticles uniformly distributed on their surface. The behavior of the defect structure of the composites during thermally stimulated hydrogen desorption and exposure to a hydrogen atmosphere at a pressure of 2 and 30 bar was characterized by positron annihilation methods. The results of in situ positron spectroscopy allow mechanisms to be established for improving the main characteristics of hydrogen storage materials, as well as for technological approaches to be developed for forming and controlling their structure. A comprehensive analysis of time correlations of the parameters of the Doppler broadening of the annihilation line, pressure, and temperature in the processes of thermal exposure, as well as the effect of a hydrogen atmosphere on the MgH_2-EEWNi composite allows the most complete data to be obtained on the sorption and desorption properties and internal structure. It has been established that the decrease in the activation energy of magnesium hydride dissociation upon the addition of nanosized nickel powder is due to the fact that the deposition of nickel nanoparticles on magnesium hydride particles reduces the binding energy of hydrogen with magnesium.

Author Contributions: Conceptualization, V.N.K., A.K. and R.S.L.; Methodology, A.K., R.R.E., N.K. and R.S.L.; Software, M.A.K. and P.I.K.; Validation, V.N.K.; Formal analysis, A.K., R.R.E., R.S.L., M.A.K., N.K. and P.I.K.; Resources, V.N.K., A.K., I.A.U. and A.V.T.; Data curation, A.K., R.R.E., I.A.U., A.V.T. and R.S.L.; Writing—original draft, A.K.; Writing—review and editing, V.N.K. and R.S.L.; Visualization, A.K. and R.R.E.; Supervision, V.N.K.; Project administration, V.N.K.; Funding acquisition, V.N.K. and R.S.L. All authors have read and agreed to the published version of the manuscript.

Funding: This research was funded by the Governmental Program, Grant No. FSWW-2023-0005.

Data Availability Statement: The raw data supporting the conclusions of this article will be made available by the authors on request.

Conflicts of Interest: The authors declare no conflicts of interest. The funders had no role in the design of the study; in the collection, analyses, or interpretation of data; in the writing of the manuscript; or in the decision to publish the results.

References

1. Bordulev, I.; Kudiiarov, V.; Svyatkin, L.; Syrtanov, M.; Stepanova, E.; Čížek, J.; Vlček, M.; Li, K.; Laptev, R.; Lider, A. Positron annihilation spectroscopy study of defects in hydrogen loaded Zr-1Nb alloy. *J. Alloys Compd.* **2019**, *798*, 685–694. [CrossRef]
2. Laptev, R.S.; Lider, A.M.; Bordulev, Y.S.; Kudiiarov, V.N.; Garanin, G.V.; Wang, W.; Kuznetsov, P.V. Investigation of defects in Hydrogen-Saturated titanium by means of positron annihilation techniques. *Defect Diffus. Forum* **2015**, *365*, 232–236. [CrossRef]
3. Laptev, R.; Lider, A.; Bordulev, Y.; Kudiiarov, V.; Garanin, G. Hydrogenation-induced microstructure changes in titanium. *J. Alloys Compd.* **2015**, *645*, S193–S195. [CrossRef]
4. Laptev, R.S.; Kudiiarov, V.N.; Bordulev, Y.S.; Mikhaylov, A.A.; Lider, A.M. Gas-phase hydrogenation influence on defect behavior in titanium-based hydrogen-storage material. *Prog. Nat. Sci. Mater. Int.* **2017**, *27*, 105–111. [CrossRef]
5. Cherdantsev, Y.P.; Chernov, I.P.; Tyurin, Y.I. *Methods for Studying Metalhydrogen Systems*; Energoatomizdat: Moscow, Russia, 2004; p. 270.
6. Faber, M.S.; Lukowski, M.A.; Ding, Q.; Kaiser, N.S.; Jin, S. Earth-Abundant metal pyrites (FeS_2, CoS_2, NiS_2, and their alloys) for highly efficient hydrogen evolution and polysulfide reduction electrocatalysis. *J. Phys. Chem. C* **2014**, *118*, 21347–21356. [CrossRef]
7. Kolachev, B.A. Hydrogen in metals and alloys. *Met. Sci. Heat Treat.* **1999**, *41*, 93–100. [CrossRef]

8. Alefeld, G.; Voelkl, J. *Hydrogen in Metals I—Basic Properties*; Springer: Berlin/Heidelberg, Germany; New York, NY, USA, 1978; Volume 28.
9. Geld, P.V.; Ryabov, R.A.; Kodes, E.S. *Hydrogen and Imperfections of Metal Structure*; Metallurgy: Moscow, Russia, 1979; 221p.
10. Popov, E.; Troev, T.; Petrov, L.; Berovski, K.; Peneva, S.; Kolev, B. Model calculations of positron interaction in materials for ITER. *Bulg. Chem. Commun.* **2015**, *47*, 192–199.
11. Gainotti, A.; Ghezzi, C.; Manfredi, M.; Zecchina, L. Positron lifetimes in metal hydrides. *Il Nuovo Cimento B* **1968**, *56*, 47–56. [CrossRef]
12. Budziak, A.; Dryzek, J.; Krawczyk, J.; Zieliński, P.M. Calorimetric and Positron Lifetime Measurements of Hydrogenated Carbon Nanocones. *Acta Phys. Pol. A* **2010**, *117*, 574–577. [CrossRef]
13. Laptev, R.S.; Bordulev, Y.S.; Kudiiarov, V.N.; Lider, A.M.; Garanin, G.V. Positron Annihilation Spectroscopy of Defects in Commercially Pure Titanium Saturated with Hydrogen. *Adv. Mater. Res.* **2014**, *880*, 134–140. [CrossRef]
14. Hautojarvi, P.; Huomo, H.; Puska, M.; Vehanen, A. Vacancy recovery and vacancy-hydrogen interaction in niobium and tantalum studied by positrons. *Phys. Review. B Condens. Matter* **1985**, *32*, 4326–4331. [CrossRef]
15. Kulkova, S. Electron and positron characteristics of group IV metal dihydrides. *Int. J. Hydrogen Energy* **1996**, *21*, 1041–1047. [CrossRef]
16. Aref'ev, K.P.; Boev, O.V.; Imas, O.N.; Lider, A.M.; Surkov, A.S.; Chernov, I.P. Annihilation of positrons in hydrogen-saturated titanium. *Phys. Solid State* **2003**, *45*, 1–5. [CrossRef]
17. Sakaki, K.; Kawase, T.; Hirato, M.; Mizuno, M.; Araki, H.; Shirai, Y.; Nagumo, M. The effect of hydrogen on vacancy generation in iron by plastic deformation. *Scr. Mater.* **2006**, *55*, 1031–1034. [CrossRef]
18. Chernov, I.P. Accumulation and elimination of hydrogen defects under radiation and heat treatment of titanium. *Fiz. Khimiya Obrab. Mater.* **2002**, *3*, 55–59.
19. Takai, K.; Shoda, H.; Suzuki, H.; Nagumo, M. Lattice defects dominating hydrogen-related failure of metals. *Acta Mater.* **2008**, *56*, 5158–5167. [CrossRef]
20. Middleburgh, S.C.; Voskoboinikov, R.E.; Guenette, M.C.; Riley, D.P. Hydrogen induced vacancy formation in tungsten. *J. Nucl. Mater.* **2014**, *448*, 270–275. [CrossRef]
21. Lin, H.-J.; Tang, J.-J.; Yu, Q.; Wang, H.; Ouyang, L.-Z.; Zhao, Y.-J.; Liu, J.-W.; Wang, W.-H.; Zhu, M. Symbiotic $CeH_{2.73}/CeO_2$ catalyst: A novel hydrogen pump. *Nano Energy* **2014**, *9*, 80–87. [CrossRef]
22. Bououdina, M.; Grant, D.; Walker, G. Review on hydrogen absorbing materials—Structure, microstructure, and thermodynamic properties. *Int. J. Hydrogen Energy* **2005**, *31*, 177–182. [CrossRef]
23. Kojima, Y. Hydrogen storage materials for hydrogen and energy carriers. *Int. J. Hydrogen Energy* **2019**, *44*, 18179–18192. [CrossRef]
24. Khafidz, N.Z. Abd. K.; Yaakob, Z.; Lim, K.L.; Timmiati, S.N. The kinetics of lightweight solid-state hydrogen storage materials: A review. *Int. J. Hydrogen Energy* **2016**, *41*, 13131–13151. [CrossRef]
25. Rusman, N.A.A.; Dahari, M. A review on the current progress of metal hydrides material for solid-state hydrogen storage applications. *Int. J. Hydrogen Energy* **2016**, *41*, 12108–12126. [CrossRef]
26. Sakintuna, B.; Lamaridarkrim, F.; Hirscher, M. Metal hydride materials for solid hydrogen storage: A review. *Int. J. Hydrogen Energy* **2007**, *32*, 1121–1140. [CrossRef]
27. Ismail, M.; Sinin, A.M.; Sheng, C.K.; Nik, W.B.W. Desorption Behaviours of Lithium Alanate with Metal Oxide Nanopowder Additives. *Int. J. Electrochem. Sci.* **2014**, *9*, 4959–4973. [CrossRef]
28. Cortez, J.J.; Castro, F.J.; Troiani, H.E.; Pighin, S.A.; Urretavizcaya, G. Kinetic improvement of H_2 absorption and desorption properties in Mg/MgH_2 by using niobium ethoxide as additive. *Int. J. Hydrogen Energy* **2019**, *44*, 11961–11969. [CrossRef]
29. Zhang, X.; Liu, Y.; Ren, Z.; Zhang, X.; Hu, J.; Huang, Z.; Lu, Y.; Gao, M.; Pan, H. Realizing 6.7 wt% reversible storage of hydrogen at ambient temperature with non-confined ultrafine magnesium hydrides. *Energy Environ. Sci.* **2020**, *14*, 2302–2313. [CrossRef]
30. Xie, X.; Chen, M.; Hu, M.; Wang, B.; Yu, R.; Liu, T. Recent advances in magnesium-based hydrogen storage materials with multiple catalysts. *Int. J. Hydrogen Energy* **2019**, *44*, 10694–10712. [CrossRef]
31. Vigeholm, B.; Kjøller, J.; Larsen, B. Magnesium for hydrogen storage. *J. Less Common Met.* **1980**, *74*, 341–350. [CrossRef]
32. Galey, B.; Auroux, A.; Sabo-Etienne, S.; Dhaher, S.; Grellier, M.; Postole, G. Improved hydrogen storage properties of Mg/MgH_2 thanks to the addition of nickel hydride complex precursors. *Int. J. Hydrogen Energy* **2019**, *44*, 28848–28862. [CrossRef]
33. Lin, H.J.; Ouyang, L.Z.; Wang, H.; Zhao, D.Q.; Wang, W.H.; Sun, D.L.; Zhu, M. Hydrogen storage properties of Mg–Ce–Ni nanocomposite induced from amorphous precursor with the highest Mg content. *Int. J. Hydrogen Energy* **2012**, *37*, 14329–14335. [CrossRef]
34. Yang, J.; Sudik, A.; Wolverton, C. Activation of hydrogen storage materials in the Li–Mg–N–H system: Effect on storage properties. *J. Alloys Compd.* **2006**, *430*, 334–338. [CrossRef]
35. Zhang, J.; Zhu, Y.; Yao, L.; Xu, C.; Liu, Y.; Li, L. State of the art multi-strategy improvement of Mg-based hydrides for hydrogen storage. *J. Alloys Compd.* **2018**, *782*, 796–823. [CrossRef]

36. Zaluska, A.; Zaluski, L.; Ström–Olsen, J.O. Nanocrystalline magnesium for hydrogen storage. *J. Alloys Compd.* **1999**, *288*, 217–225. [CrossRef]
37. Lyu, J.; Lider, A.; Kudiiarov, V. Using ball milling for modification of the Hydrogenation/Dehydrogenation process in Magnesium-Based hydrogen storage materials: An overview. *Metals* **2019**, *9*, 768. [CrossRef]
38. Zaluska, A.; Zaluski, L.; Ström-Olsen, J.O. Synergy of hydrogen sorption in ball-milled hydrides of Mg and Mg_2Ni. *J. Alloys Compd.* **1999**, *289*, 197–206. [CrossRef]
39. Malka, I.E.; Czujko, T.; Bystrzycki, J. Catalytic effect of halide additives ball milled with magnesium hydride. *Int. J. Hydrogen Energy* **2009**, *35*, 1706–1712. [CrossRef]
40. Zadorozhnyy, V.Y.; Klyamkin, S.N.; Zadorozhnyy, M.Y.; Strugova, D.V.; Milovzorov, G.S.; Louzguine-Luzgin, D.V.; Kaloshkin, S.D. Effect of mechanical activation on compactibility of metal hydride materials. *J. Alloys Compd.* **2016**, *707*, 214–219. [CrossRef]
41. Huot, J.; Liang, G.; Schulz, R. Mechanically alloyed metal hydride systems. *Appl. Phys. A* **2001**, *72*, 187–195. [CrossRef]
42. Wu, C.Z.; Wang, P.; Yao, X.; Liu, C.; Chen, D.M.; Lu, G.Q.; Cheng, H.M. Effect of carbon/noncarbon addition on hydrogen storage behaviors of magnesium hydride. *J. Alloys Compd.* **2005**, *414*, 259–264. [CrossRef]
43. Oelerich, W.; Klassen, T.; Bormann, R. Metal oxides as catalysts for improved hydrogen sorption in nanocrystalline Mg-based materials. *J. Alloys Compd.* **2001**, *315*, 237–242. [CrossRef]
44. Milošević, S.; Kurko, S.; Pasquini, L.; Matović, L.; Vujasin, R.; Novaković, N.; Novaković, J.G. Fast hydrogen sorption from MgH_2–VO_2(B) composite materials. *J. Power Sources* **2016**, *307*, 481–488. [CrossRef]
45. Polanski, M.; Bystrzycki, J. Comparative studies of the influence of different nano-sized metal oxides on the hydrogen sorption properties of magnesium hydride. *J. Alloys Compd.* **2009**, *486*, 697–701. [CrossRef]
46. Shao, H.; Asano, K.; Enoki, H.; Akiba, E. Preparation and hydrogen storage properties of nanostructured Mg–Ni BCC alloys. *J. Alloys Compd.* **2008**, *477*, 301–306. [CrossRef]
47. Liu, H.; Wang, Z.; Zhang, J.; Tao, B.; Liu, Q. Recent advances in hydrogen storage of MgH_2 doped by Ni. *IOP Conf. Ser. Earth Environ. Sci.* **2019**, *267*, 022042. [CrossRef]
48. Shao, H.; Xu, H.; Wang, Y.; Li, X. Synthesis and hydrogen storage behavior of Mg–Co–H system at nanometer scale. *J. Solid State Chem.* **2004**, *177*, 3626–3632. [CrossRef]
49. Pukazhselvan, D.; Nasani, N.; Yang, T.; Bdikin, I.; Kovalevsky, A.V.; Fagg, D.P. Dehydrogenation Properties of Magnesium Hydride Loaded with Fe, Fe−C, and Fe−Mg Additives. *ChemPhysChem* **2016**, *18*, 287–291. [CrossRef]
50. Zhou, C.; Zhang, J.; Bowman, R.C.; Fang, Z.Z. Roles of TI-Based Catalysts on magnesium hydride and its hydrogen storage properties. *Inorganics* **2021**, *9*, 36. [CrossRef]
51. Ren, C.; Fang, Z.Z.; Zhou, C.; Lu, J.; Ren, Y.; Zhang, X. Hydrogen Storage Properties of Magnesium Hydride with V-Based Additives. *J. Phys. Chem. C* **2014**, *118*, 21778–21784. [CrossRef]
52. Liu, Y.; Zhu, J.; Liu, Z.; Zhu, Y.; Zhang, J.; Li, L. Magnesium nanoparticles with PD decoration for hydrogen storage. *Front. Chem.* **2020**, *7*, 949. [CrossRef]
53. Liu, Y.; Huang, Z.; Gao, X.; Wang, Y.; Wang, F.; Zheng, S.; Guan, S.; Yan, H.; Yang, X.; Jia, W. Effect of novel La-based alloy modification on hydrogen storage performance of magnesium hydride: First-principles calculation and experimental investigation. *J. Power Sources* **2022**, *551*, 232187. [CrossRef]
54. Spassov, T.; Lyubenova, L.; Köster, U.; Baró, M.D. Mg–Ni–RE nanocrystalline alloys for hydrogen storage. *Mater. Sci. Eng. A* **2004**, *375–377*, 794–799. [CrossRef]
55. Rahmalina, D.; Rahman, R.A.; Suwandi, A.; Ismail, N. The recent development on MgH_2 system by 16 wt% nickel addition and particle size reduction through ball milling: A noticeable hydrogen capacity up to 5 wt% at low temperature and pressure. *Int. J. Hydrogen Energy* **2020**, *45*, 29046–29058. [CrossRef]
56. Xie, L.-S.; Li, J.-S.; Zhang, T.-B.; Kou, H.-C. Role of milling time and Ni content on dehydrogenation behavior of MgH_2/Ni composite. *Trans. Nonferrous Met. Soc. China* **2017**, *27*, 569–577. [CrossRef]
57. Amama, P.B.; Grant, J.T.; Spowart, J.E.; Shamberger, P.J.; Voevodin, A.A.; Fisher, T.S. Catalytic influence of Ni-based additives on the dehydrogenation properties of ball milled MgH_2. *J. Mater. Res.* **2011**, *26*, 2725–2734. [CrossRef]
58. Rahmalina, D.; Rahman, R.A.; Ismail, I. Experimental evaluation for the catalytic effect of nickel in micron size on magnesium hydride. *Wseas Trans. Appl. Theor. Mech.* **2021**, *16*, 293–302. [CrossRef]
59. Varin, R.A.; Czujko, T.; Wasmund, E.B.; Wronski, Z.S. Catalytic effects of various forms of nickel on the synthesis rate and hydrogen desorption properties of nanocrystalline magnesium hydride (MgH_2) synthesized by controlled reactive mechanical milling (CRMM). *J. Alloys Compd.* **2006**, *432*, 217–231. [CrossRef]
60. Doppiu, S.; Schultz, L.; Gutfleisch, O. In situ pressure and temperature monitoring during the conversion of Mg into MgH_2 by high-pressure reactive ball milling. *J. Alloys Compd.* **2006**, *427*, 204–208. [CrossRef]
61. Liang, G.; Huot, J.; Boily, S.; Van Neste, A.; Schulz, R. Catalytic effect of transition metals on hydrogen sorption in nanocrystalline ball milled MgH_2–Tm (Tm=Ti, V, Mn, Fe and Ni) systems. *J. Alloys Compd.* **1999**, *292*, 247–252. [CrossRef]

62. Shang, C. Mechanical alloying and electronic simulations of (MgH_2+M) systems (M=Al, Ti, Fe, Ni, Cu and Nb) for hydrogen storage. *Int. J. Hydrogen Energy* **2003**, *29*, 73–80. [CrossRef]
63. Ilyin, A.P.; Mostovshchikov, A.V.; Nazarenko, O.B.; Zmanovskiy, S.V. Heat release in chemical reaction between micron aluminum powders and water. *Int. J. Hydrogen Energy* **2019**, *44*, 28096–28103. [CrossRef]
64. Mostovshchikov, A.; Gubarev, F.; Chumerin, P.; Arkhipov, V.; Kuznetsov, V.; Dubkova, Y. Solid energetic material based on aluminum micropowder modified by microwave radiation. *Crystals* **2022**, *12*, 446. [CrossRef]
65. Mostovshchikov, A.; Gubarev, F.; Nazarenko, O.; Pestryakov, A. Influence of Short-Pulse microwave radiation on thermochemical properties Aluminum micropowder. *Materials* **2023**, *16*, 951. [CrossRef]
66. Mostovshchikov, A.V.; Goldenberg, B.G.; Nazarenko, O.B. Effect of synchrotron radiation on thermochemical properties of aluminum micro- and nanopowders. *Mater. Sci. Eng. B* **2022**, *285*, 115961. [CrossRef]
67. Kudiiarov, V.N.; Kurdyumov, N.; Elman, R.R.; Svyatkin, L.A.; Terenteva, D.V.; Semyonov, O. Microstructure and hydrogen storage properties of MgH_2/MIL-101(Cr) composite. *J. Alloys Compd.* **2023**, *976*, 173093. [CrossRef]
68. Bordulev, I.; Laptev, R.; Kudiiarov, V.; Elman, R.; Popov, A.; Kabanov, D.; Ushakov, I.; Lider, A. Positron annihilation spectroscopy complex for structural defect analysis in Metal–Hydrogen systems. *Materials* **2022**, *15*, 1823. [CrossRef]
69. Kudiiarov, V.; Elman, R.; Kurdyumov, N.; Laptev, R. The phase transitions behavior and defect structure evolution in magnesium hydride/single-walled carbon nanotubes composite at hydrogen sorption-desorption processes. *J. Alloys Compd.* **2023**, *953*, 170138. [CrossRef]
70. Kudiiarov, V.N.; Kurdyumov, N.; Elman, R.R.; Laptev, R.S.; Kruglyakov, M.A.; Ushakov, I.A.; Tereshchenko, A.V.; Lider, A.M. The defect structure evolution in magnesium hydride/metal-organic framework structures MIL-101 (Cr) composite at high temperature hydrogen sorption-desorption processes. *J. Alloys Compd.* **2023**, *966*, 171534. [CrossRef]
71. Kudiiarov, V.N.; Kenzhiyev, A.; Mostovshchikov, A.V. Improvement of the Hydrogen Storage Characteristics of MgH_2 with Al Nano-Catalyst Produced by the Method of Electric Explosion of Wires. *Materials* **2024**, *17*, 639. [CrossRef]